Plasmons

DOI: 10.1002/anie.201000972

Response of Molecular Junctions to Surface Plasmon Polaritons**

*Gilad Noy, Ayelet Ophir, and Yoram Selzer**

Surface plasmons are coherent oscillations of conductive electrons that occur in a skin layer of metal and are capable of producing strong local electromagnetic fields in the near-field region.[1] Plasmons are imperative in surface-enhanced Raman[2–5] and fluorescence spectroscopy[6] as they significantly boost the sensitivity of these methods for the detection of dilute concentrations of analyte molecules. Plasmons can be coupled to molecular resonances,[7,8] or molecules can be exploited to control the properties of plasmons and the optical properties of nanoscale metal structures upon irradiation.[9] These studies, as well as several theoretical results,[10] suggest that plasmons should also affect the transport properties of molecular junctions. Several recently reported experimental approaches towards this goal are based on the average effect from a large number of junctions formed in ordered arrays of metal nanoparticles interlinked with molecules.[11] Herein we report the current response of individual well-defined molecular junctions to surface plasmons. The observed enhancement of current is explained by a photon-assisted tunneling mechanism.

"Suspended-wire" molecular junctions (SWMJs) were fabricated by trapping Au or Ag nanowires, which were capped with a self-assembled monolayer of either 1,9-nonanedithiol (C9) or decanethiol (C10) onto lithographically defined Au leads by using a dielectrophoresis technique (see Figure 1 and the Supporting Information). Figure 1a shows representative *I–V* curves of junctions based on the two molecules. Transition voltage spectroscopy (TVS) and inelastic electron tunneling spectroscopy (IETS) measurements were taken in order to confirm the molecular nature of the junctions. TVS measurements are interpreted with a Fowler–Nordheim analysis, that is, plots of $\ln(I/V^2)$ versus $1/V$, which reveal minimum points at transition-voltage (V_T) values that are characteristic of the molecules under investigation.[12] Figure 1b shows typical TVS curves of junctions with C9 molecules. An average value of $V_T = (1.1 \pm 0.07)$ V was calculated from all (C9 + C10) junctions. IETS measurements were taken at 5 K using a standard lock-in technique (Figure 1c), which revealed typical alkane vibrations in both bias polarities.[13] The agreement of measured V_T values with previous results,[14] and the lack of shift in the IETS peaks (within an error of ± 2 mV) prove that there is no potential divider in the suspended structures, that is, although the nanowires that are completely covered with a molecular layer could potentially form two molecular junctions in each SWMJ, only one junction per suspended nanowire (and a metal to metal contact on the other end) is formed.

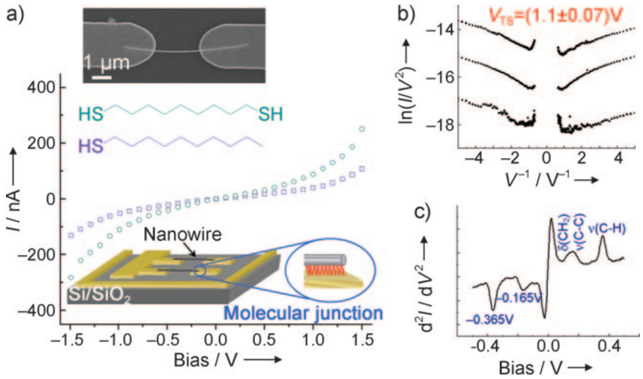

Figure 1. a) Representation of a "suspended-wire" molecular junction and typical *I–V* curves of the molecules used in this study. Inset: SEM image of a suspended nanowire. b) Transition voltage spectroscopy of three different C9 junctions. c) Representative IETS measurements of a C9 junction measured at 5 K, showing characteristic peaks of alkyl chains (C10 junctions have similar peaks).

Laser irradiation of selected junctions under ambient conditions was carried out by using a microscope with maximum intensity of approximately 6 mW µm^{-2} and laser polarization parallel to the nanowires. Two wavelengths were used (see below): 781 nm (1.58 eV) and 658 nm (1.88 eV). We estimate the temperature increment under the lasers, which operated at maximum intensity, to be not more than $\Delta T =$ 5 K. This estimate is based on the resistance change of the suspended-wire structures with bare metal nanowires; we observed ohmic behavior that changes as a function of temperature according to $R = R_0(1+\beta\Delta T)$, where β is the temperature coefficient of the metal and R and R_0 are the resistances with and without irradiation, respectively.

The SWMJ showed a maximum current increase of two times over a bath temperature range of 300–400 K. Upon a temperature change of 5 K, which arose from the laser irradiation, the current change was negligible (see the Supporting Information). We discarded all data that showed conductivity changes below twofold upon irradiation, thus leaving a substantial margin in terms of the exact effective temperature of the conducting junctions.

Only one end of the junction in the suspended structure was found to be responsive to irradiation. Finite-difference time-domain (FDTD) simulations provided a better insight into the role of plasmons in the SWMJs (Figure 2). Propagat-

[*] G. Noy,[+] A. Ophir,[+] Dr. Y. Selzer
School of Chemistry, Tel Aviv University
Ramat Aviv, Tel Aviv 69978 (Israel)
Fax: (+972) 3-640-7362
E-mail: selzer@post.tau.ac.il

[+] These authors contributed equally to this work.

[**] Support by the Israel Science Foundation through grant numbers 1507/09 and 1274/09 and through a "Converging Technologies" fellowship to G.N. is gratefully acknowledged.

Supporting information for this article is available on the WWW under http://dx.doi.org/10.1002/anie.201000972.

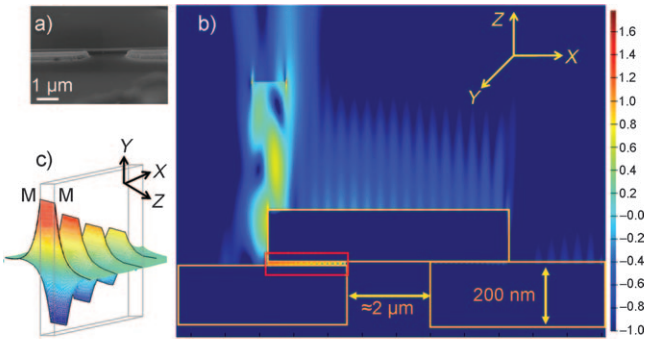

Figure 2. a) SEM side view of a SWMJ. b) FDTD simulation of the field intensity in a SWMJ, calculated for $\lambda = 781$ nm. The spatial scales in the z and x directions are different. The color scale of the field intensity is in arbitrary units. Laser light impinges on the left side of the nanowire, where the junction is located (marked by a red rectangle). The electric field is enhanced in the junction. A plasmon propagates along the nanowire to the other side of the structure. c) Geometry and characteristic tangential (between metals, M) electric-field (Ez) profile for the junction (note the different coordination system relative to (b). The Ez is enhanced at the entrance by a factor of ca. 100, fluctuates with a characteristic plasmon wavelength of ca. 50 nm, and is attenuated to zero after propagating ca. 1 µm in the x direction (see also the red color all along the junction in b).

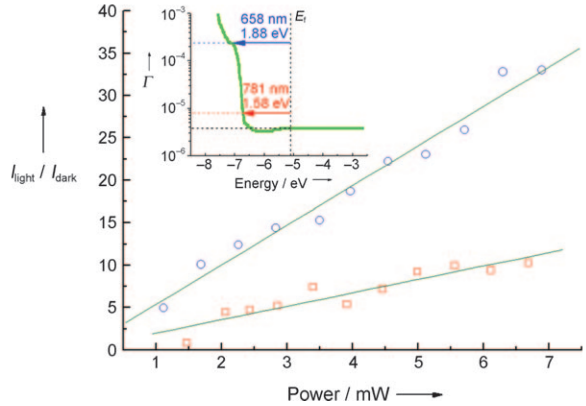

Figure 3. Measured I_{light}/I_{dark} ratio for a Au–C9–Au junction as a function of laser power, using two wavelengths 658 nm (blue circles), and 781 nm (red rectangles). The continuous green lines are a guide. Inset: Calculated transmission probability Γ through the junction as a function of energy. The arrows show that $\Gamma(E_f - 1.58\text{ eV}) \approx 5\,\Gamma(E_f)$ and that $\Gamma(E_f - 1.88\text{ eV}) \approx 100\,\Gamma(E_f)$.

ing surface plasmons can be launched in a nanowire only when the excitation laser is incident on the end of the nanowire.[15] The dispersion curves of metal–insulator–metal structures, with insulator thicknesses and dielectric parameters similar to the molecules used in this study, were recently calculated.[16] These results show that propagating plasmons can be launched into the junctions by only a limited range of photon energy values. The 781 nm and 658 nm wavelengths fall within this range, and result in propagating plasmons in the junctions with characteristic wavelengths of approximately 50 nm and propagation length of several hundreds of nanometers. Thus, a substantial length of each junction (which is typically less than 1 µm, see Figures 1 and 2) is affected by the plasmons.

The main results for a Au–C9–Au junction are summarized in Figure 3, which shows the ratio between the optically induced current I_{light} and the current without irradiation I_{dark} as a function of laser intensity for two wavelengths at a bias value of 1 mV (see the Supporting Information for details on the distribution of results and how each point was measured and calculated). Two main observations are apparent: the ratio I_{light}/I_{dark} increases linearly with laser intensity and has a higher value for $\lambda = 658$ nm. The distribution of results from the different junctions is within $\pm 50\%$ (error bars are not shown for clarity).

The experimental observations can be explained semi-quantitatively by a photon-assisted tunneling mechanism[10b,j] using an analytical expression from the treatment of Tien and Gordon.[17] According to this model, in addition to the applied dc bias, there is also a time-varying potential across the gap, induced in this case by the propagating plasmons (see Figure 2c). Under these conditions a certain fraction of the tunneling charges undergo inelastic tunneling events in which they either emit ($n < 0$) or absorb ($n > 0$) photons with energy $\hbar\omega$ by interacting with the oscillating (plasmon) field. According to this model, the energy-dependent transmission rate across a junction under the effect of an oscillatory potential becomes:

$$\Gamma(E) = \sum_n J_n^2\left(\frac{eV_\omega}{\hbar\omega}\right)\Gamma(E + n\hbar\omega) \qquad (1)$$

where $\Gamma(E)$ and $\Gamma(E+n\hbar\omega)$ are the transmission rate with and without irradiation, respectively, and $J_n(\alpha)$ is an n order Bessel function with $\alpha = eV_\omega/\hbar\omega$ where V_ω is the effective amplitude of the oscillating potential formed by the plasmon in the junction.

The calculated electric profile along the cross section of the junctions (between the metal nanowires and gold leads) is shown in Figure 2c. The plasmonic enhancement of the electric field on the molecules is in the order of approximately 100 times. Considering the laser intensities used in these experiments, the vacuum propagating electric field is in the order of 2 mV nm^{-1}. After enhancement, the field is $E_z \approx 200\text{ mV nm}^{-1}$ inside the junctions. Deep inside the metal, within an order of few skin depths, which for Au at 781 nm and 658 nm is approximately 25 nm, the field is zero. Any electron that is within the metal and moves towards the interface within a distance of a mean free path (taken here as $l = 10$ nm) contributes to the tunneling process and is also influenced by the oscillating field. Therefore, V_ω $(=El)$ is approximately 2 V. This value can be used to estimate a value of α for the two wavelengths: $\alpha_{658} \approx 1.06$, $\alpha_{781} \approx 1.25$. With the laser intensities used in these experiments, the contribution of multi-photon processes is negligible, and therefore we need to consider only the J_0 and J_1 Bessel functions in Equation (1).

The transmission probability through molecular junctions based on thiolated alkyl chains, and also their density of states have been theoretically calculated by several research groups.[18] We used this data to estimate $\Gamma(E_f \pm \hbar\omega)$, where E_f is the Fermi energy (Figure 3, inset). The highest occupied molecular orbital (HOMO) level in the alkyl chains is closer to E_f than the lowest unoccupied molecular orbital (LUMO). Therefore, as a first approximation for the wavelengths used here $\Gamma(E_f) \approx \Gamma(E_f+1.58\,\text{eV}) \approx \Gamma(E_f+1.88\,\text{eV})$, while $\Gamma(E_f-1.58\,\text{eV})$ is higher than $\Gamma(E_f)$ by an order of magnitude, and $\Gamma(E_f-1.88\,\text{eV})$ by two orders of magnitude. Use of the transmission enhancement and the above α values in Equation (1) gives a I_{light}/I_{dark} ratio (at maximum intensity) of 5 and 40 for $\lambda = 781$ nm and $\lambda = 658$ mn, respectively. These values are consistent with the experimental results. We note that without molecules (C9 and C10), that is, if the barrier for tunneling is approximately the work function of the metal, current enhancement by plasmons requires photons with energies of approximately 5 eV. These photons are expected to be absorbed by the metal as their energy is beyond the plasma energy (ca. 2.4 eV).

In conclusion, we have demonstrated the effect of plasmons on the conductivity of molecular junctions by using SWMJs, which are a new type of molecular junction. The observed current enhancement is in semiquantitative agreement with a photon-assisted tunneling mechanism and numerical simulations of the plasmon-induced enhancement of the electromagnetic field between the metal leads of the junctions. Further work to elucidate the effect of attributes such as molecular structure and potential bias is underway.

Received: February 16, 2010
Published online: July 6, 2010

Keywords: molecular junctions · nanostructures · plasmons · tunneling

[1] a) S. A. Maier, H. A. Atwater, *J. Appl. Phys.* **2005**, *98*, 011101; b) W. L. Barnes, A. Dereux, T. W. Ebbesen, *Nature* **2003**, *424*, 824–830.
[2] a) M. Moskovits, *Rev. Mod. Phys.* **1985**, 57, 783; b) K. A. Willets, R. P. Van Duyne, *Annu. Rev. Phys. Chem.* **2007**, *58*, 267.
[3] X. Chen, A. B. Braunschweig, M. J. Wiester, S. Yeganeh, M. A. Ratner, C. A. Mirkin, *Angew. Chem.* **2009**, *121*, 5280–5283; *Angew. Chem. Int. Ed.* **2009**, *48*, 5178–5181.
[4] T. Shamai, Z. Ioffe, A. Ophir, G. Noy, I. Yutsis, K. Kfir, O. Cheshnovsky, Y. Selzer, *Nat. Nanotechnol.* **2008**, *3*, 727–732.
[5] D. R. Ward, N. K. Grady, C. S. Levin, N. J. Halas, Y. Wu, P. Nordlander, D. Natelson, *Nano Lett.* **2007**, *7*, 1396–1400.
[6] A. Kinkhabwala, Z. Yu, S. Fan, Y. Avlasevich, K. Mullen, W. E. Moerner, *Nat. Photonics* **2009**, *3*, 654–657.
[7] A. Salomon, C. Genet, T. W. Ebbesen, *Angew. Chem.* **2009**, *121*, 8904–8907; *Angew. Chem. Int. Ed.* **2009**, *48*, 8748–8751.
[8] W. Ni, T. Ambjrnsson, S. P. Apell, H. Chen, J. Wang, *Nano Lett.* **2010**, *10*, 77–84.
[9] a) D. Neuhauser, K. Lopata, *J. Chem. Phys.* **2007**, *127*, 154715–154725; b) A. Mayer, G. Schatz, *J. Phys. Condens. Matter* **2009**, *21*, 325301; c) S. J. Park, R. E. Palmer, *Phys. Rev. Lett.* **2009**, *102*, 216805.
[10] a) G. Q. Li, M. Schreiber, U. Kleinekathöfer, *Eur. Phys. Lett.* **2007**, *79*, 27006; b) J. K. Viljas, F. Pauly, J. C. Cuevas, *Phys. Rev. B* **2008**, *77*, 155119; c) J. Lehmann J, S. Camalet, S. Kohler, P. Hänggi, *Chem. Phys. Lett.* **2003**, *368*, 282; d) J. Lehmann J, S. Kohler, P. Hänggi P, A. Nitzan, *Phys. Rev. Lett.* **2002**, *88*, 228305; e) M. Galperin, A. Nitzan, *Phys. Rev. Lett.* **2005**, *95*, 206802; f) M. Galperin, A. Nitzan, M. A. Ratner, *Phys. Rev. Lett.* **2006**, *96*, 166803; g) A. Keller, O. Atabek, M. A. Ratner, V. Mujica, *J. Phys. B* **2002**, *35*, 4981; h) I. Urdaneta, A. Keller, O. Atabek, V. Mujica, *Int. J. Quantum Chem.* **2004**, *99*, 460; i) A. Tikhonov, R. D. Coalson, Y. Dahnovsky, *J. Chem. Phys.* **2002**, *117*, 567; j) I. Urdaneta, A. Keller, O. Atabek, V. Mujica, *J. Chem. Phys.* **2007**, *127*, 154110.
[11] a) H. Nakanishi, K. J. M. Bishop, B. Kowalczyk, A. Nitzan, E. A. Weiss, K. V. Tretiakov, M. M. Apocada, R. Klajn, J. F. Stoddart, B. A. Grzybowski, *Nature* **2009**, *460*, 371–375; b) S. J. Van der Molen, J. Liao, T. Kudernac, J. S. Agustsson, L. Bernard, M. Calame, B. J. Van Wees, B. L. Feringa, C. Schönenberger, *Nano Lett.* **2009**, *9*, 76–80; c) M. A. Mangold, C. Weiss, M. Calame, A. W. Holleitner, *Appl. Phys. Lett.* **2009**, *94*, 161104; d) P. Banerjee, D. Conklin, S. Nanayakkara, T. H. Park, M. J. Therien, D. A. Bonnell, *ACS Nano* **2010**, *4*, 1019.
[12] J. M. Beebe, B. Kim, J. W. Gadzuk, C. D. Frisbie, J. G. Kushmerick, *Phys. Rev. Lett.* **2006**, *97*, 026801.
[13] N. Okabayashi, Y. Konda, T. Komeda, *Phys. Rev. Lett.* **2008**, *100*, 217801.
[14] J. M. Beebe, B. Kim, C. D. Frisbie, J. G. Kushmerick, *ACS Nano* **2008**, *2*, 827.
[15] A. W. Sanders, D. A. Routenberg, B. J. Wiley, Y. Xia, E. R. Dufresne, M. A. Reed, *Nano Lett.* **2006**, *6*, 1822.
[16] H. T. Miyazaki, Y. Kurokawa, *Phys. Rev. Lett.* **2006**, *96*, 097401; H. T. Miyazaki, Y. Kurokawa, *Phys. Rev. B* **2007**, *75*, 035411.
[17] P. Tien, J. Gordon, *Phys. Rev.* **1963**, *129*, 647.
[18] a) W. Haiss, S. Martin, L. E. Scullion, L. Bouffier, S. J. Higgins, R. J. Nichols, *Phys. Chem. Chem. Phys.* **2009**, *11*, 10831–10838; b) J. M. Seminario, L. Yan, *Int. J. Quantum Chem.* **2005**, *102*, 711; c) G. C. Solomon, D. Q. Andrews, R. P. Van Duyne, M. A. Ratner, *J. Am. Chem. Soc.* **2008**, *130*, 7788–7789.

